

Abutment Reactions and Higher Modes of Transverse Vibration of Continuous Bridges



15 WCEE
LISBOA 2012

G. Della Corte & R. De Risi

Department of Structural Engineering, University of Naples Federico II, Italy

SUMMARY:

The paper discusses the problem of predicting abutment reactions of continuous bridges through a simplified method of analysis based on the response spectrum method. The feasibility of substituting the real discrete support system with a continuous (Winkler) spring system is discussed. Limitations of this approach are evaluated by comparing the approximate solution with the theoretical correct one, which is evaluated through numerical finite element model analysis. Both linear and nonlinear system response is addressed. The comparison shows that the Winkler simplification is good in case of sufficiently small intermediate support stiffness (e.g. in case of deck isolation) and/or large number of spans. However, there will always be an upper bound to the intermediate support stiffness beyond which the error linked to the Winkler model will start to increase significantly becoming unacceptably large.

Keywords: Analysis, bridges, design, energy dissipation, isolation

1. INTRODUCTION

Transverse vibrations of continuous bridges can be assimilated to those of continuous beams on flexible supports. To reduce transmission of seismic forces to substructures, the deck is frequently isolated by using specific isolation and/or energy dissipation systems. A special case is represented by partially-isolated bridges where the deck is isolated for transverse motion only at intermediate pier supports while it is fixed at the abutments. This design option may be found advantageous in order to eliminate the need for transverse displacement joints at the abutments. Partial isolation makes the deck displacement pattern non uniform and requires to account explicitly for the deck flexibility. A great deal of research studies and codification (AASHTO, 2010; CEN, 2005) is mainly concerned with fully-isolated bridges while some recent research efforts have been addressed to cover also the alternative of partial isolation (Tsai, 2008, Tubaldi and Dall'Asta, 2011). Partial isolation makes the bridge deck transverse motion similar to that of a continuous beam with intermediate flexible supports and fixed at the abutments. Abutment reactions play a key role in this system, both because they implicitly affect deck displacements and because they are needed in order to design end restrains and abutment foundations. This paper discusses one possibility to simplify the analysis of such bridge types by substituting the real discrete pier-isolator subsystem reactions by a continuous Winkler-type elastic reaction system. Previous results from nonlinear analysis of five case studies (Della Corte *et al.*, 2012) has clearly highlighted that abutment reactions are (i) significantly affected by higher modes of vibration and (ii) accurately evaluated by the Winkler simplification if the effective stiffness of pier isolator subsystems is sufficiently small. For larger stiffness underestimation of such reactions generally occurs. The level of underestimation depends on the relative pier/isolator-to-deck stiffness and on the number of spans.

Though the objective of the study is to establish the feasibility of using the simplified method of analysis for isolation systems, the discussion is general and the results are valid also for non isolated bridges.

2. OUTLINE OF A SIMPLIFIED METHOD OF ANALYSIS

A simplified method for transverse response analysis of multi-span continuous bridges with isolation bearings at intermediate piers and laterally restrained at the abutments has been presented in Della Corte *et al.* (2012). The method is based on the assumption that the actual displacement pattern of the deck can be approximated as the summation of a finite number of sinusoidal contributions. The amplitude of each contribution is determined from the response spectrum based on an effective period of vibration and damping ratio. The latter are evaluated per each sinusoidal “mode of vibration”. The approximation of sinusoidal modes of vibrations holds true in case of an infinite number of intermediate supports with given stiffness per unit length, i.e. for a beam on elastic Winkler-type support. Therefore, it is expected that the method converges to the real solution in case of a large number of spans, i.e. a large number of intermediate supports. However, it is also noted that in case of isolated bridges, the intermediate support stiffness is generally very small in case of a full activation of the isolation system. Therefore, the method may work well also for a limited number of spans, but with a small effective stiffness of the intermediate supports. In this Section, the simplified analysis procedure is summarised. An evaluation of the limitations linked to the sinusoidal representation of the displacement patterns, i.e. to the Winkler model, is discussed at subsequent Sections.

Figure 1 illustrates schematically the basics of the adopted calculation procedure using the spectral acceleration (S_a) vs. spectral displacement (S_d) representation. The calculation process is iterative and follows the fundamental steps outlined hereafter: 1) starting with the initial stiffness (i.e. frequency, ω_0^2) and damping ratio (ξ_0), the first trial displacement demand is obtained from the corresponding spectrum; 2) effective stiffness and damping ratio (linearized system properties) corresponding to the trial displacement are calculated; 3) using the effective stiffness a new estimate of the displacement demand is obtained from the demand spectrum corresponding to the effective damping ratio; 4) the process is repeated until sufficiently small differences are obtained for the displacement (S_{dd}) and/or force (S_{ad}) demand between two subsequent iterations.

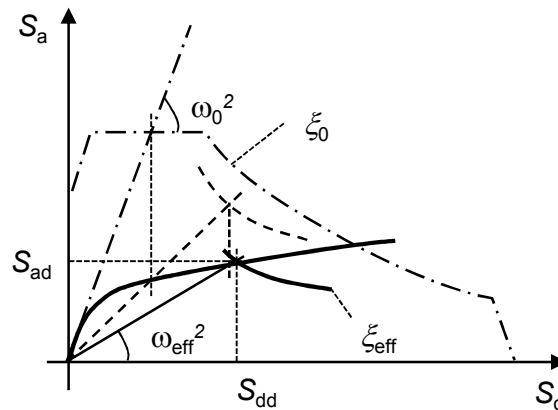


Figure 1. Outline of the calculation procedure for the n -th contribution to the displacement pattern.

The method outlined in Figure 1 is quite well established for the simplified design/analysis of nonlinear structures. The assumption of one mode of vibration dominating the response is usually made (Priestley *et al.*, 2007) and the capacity curve (bold continuous line in Figure 1) is generally obtained by means of static nonlinear analysis of finite element models, under the action of pre-fixed lateral force patterns. One aspect that has been recently given more emphasis is how to consider the contribution of higher modes of vibration. Following the former proposal in Chopra and Goel (2002), a specific study for bridges was presented in Paraskeva and Kappos (2010).

In order to calculate the effective stiffness, forces developing into the (generally) nonlinear isolation devices are required to be calculated for a given (trial) displacement. However, the total deck seismic force (V_d) is the sum of the intermediate reactions and abutment reactions. The latter are not directly

linked to the displacements, which are assumed to be zero at the abutments. In order to calculate abutment reactions, consistently with the assumption of a sinusoidal displacement pattern, the following Equation can be derived from analysis of a Winkler beam:

$$R_{ab,n} = x_n V_{d,n} = \left[1 / \left(1 + \frac{4}{\pi^4 n^4} \lambda_n^4 \right) \right] M_{eff,n} S_{a,n} \quad (1)$$

where, with reference to the n -th vibration mode: $\lambda_n = \sqrt[4]{k_{w,n} / (4EI/L^4)}$, $k_{w,n}$ = the Winkler stiffness per unit length, EI = flexural stiffness of deck, L = length of deck, $M_{eff,n}$ = effective (participating) modal mass, $S_{a,n}$ = spectral (pseudo-)acceleration.

Once end abutment and intermediate pier reactions have been calculated, the resultant of seismic deck forces is obtained and consequently the effective system stiffness can also be calculated for a given trial displacement demand (Fig. 1).

In order to calculate the effective damping ratio, the ductility demand to any intermediate isolation/energy dissipation system is calculated for any given trial displacement demand. The effective damping ratio of isolation bearings located on a pier is calculated by means of the following Equation (2), which is written assuming a bilinear approximation to the device lateral force displacement response:

$$\xi_{eff,is} = \rho (2/\pi) \sum_j 1 / \left(1 + K_{2,is}^j \Delta_{pl}^j / V_1^j \right) \quad (2)$$

where: j is the generic isolation bearing located on a pier; $\rho = (\mu - 1) / (\mu + 1)$, μ = pier-isolator subsystem ductility demand, V_1^j = shear force producing inelastic behaviour of the j -th isolator, $\Delta_{pl} = \Delta_{max} - \Delta_1^j$ = inelastic displacement demand (Δ_1^j = pier-isolator subsystem displacement corresponding to V_1^j), $K_{2,is}^j$ = stiffness corresponding to the second slope of the bilinear schematization. The reduction factor ρ is introduced to take into account that the Jacobsen's rule, which is implemented into Equation (2), generally overestimates damping (Dwairi and Kowalsky, 2004). The factor proposed is empirical and derived based on a limited number of analyses, some of which are reported in Della Corte *et al.* (2012). The effective damping ratio due to isolation bearings is added to the one from the supporting pier (by weighting the contributions based on the relative displacements). Finally the total system damping ratio is obtained by summing up contributions from the pier-isolator subsystems and the deck (by weighting the individual contributions with the work done by corresponding forces through maximum displacements) (Priestley *et al.* 2007).

3. ANALYSIS OF LINEAR MODELS

The approximations of the Winkler model have been investigated by comparing its predictions with results from numerical analysis of finite element models of continuous beams with discrete intermediate supports of equal stiffness. A comparison between the Winkler model and the real solution is presented in Makris *et al.* (2010) with reference to the first-mode period of vibration. This Section will present a similar comparison but with reference to multiple modes of vibration and abutment reactions.

Abutment reactions are normalized by means of the reactions that would develop into a simply supported beam having the same length and flexural stiffness as the continuous deck model. The normalized abutment reactions are evaluated for many modes of vibration and they are plotted versus a normalized measure of the intermediate support stiffness. The latter can be identified starting with the analysis of the Winkler model. In such a model, because of the coincidence of mode shapes of the

Winkler and simply supported beams, the relationship between the periods of vibration and the abutment reactions in the n -th mode is given by the following Equation (3), which includes the result presented in Equation (1):

$$\frac{R_{ab,n}^W}{R_{ab,n}^{SS}} = \left(\frac{T_n^W}{T_n^{SS}} \right)^2 \frac{S_a(T_n^W)}{S_a(T_n^{SS})} = \frac{1}{1 + \frac{4}{\pi^4 n^4} \lambda^4} \frac{S_a(T_n^W)}{S_a(T_n^{SS})} \quad (3)$$

The parameter λ has been previously defined (Eq. 1), but now it is independent of the mode number n because the discussion is for the simpler case of uniform support stiffness. The parameter λ is the normalized measure of the intermediate support stiffness in case of a Winkler beam. In case of a continuous beam of total length L with n_s equal spans and $(n_s - 1)$ intermediate supports of equal stiffness k , the corresponding Winkler distributed stiffness may be defined as $k_{w,s} = (n_s - 1)k/L$. The subscript s is explicitly introduced to note that for a given value of the real support stiffness the Winkler stiffness per unit length depends on the number of intermediate supports or equivalently on the number of spans n_s . This correspondence between the Winkler model stiffness per unit length and the concentrated support stiffness is obviously arbitrary and conventional, but it is frequently used in the form presented above which is adopted to make hereafter a comparison of the two models. Using the definition of λ , the normalized measure of the single support stiffness can be defined as $\kappa = \lambda_s^4 / 2(n_s - 1) = k_{w,s} / 8EI/L^4 = kL^3 / 8EI$. The coefficient 2 at the denominator is introduced to make the parameter identical to the one presented in Makris *et al.* (2010) thus favouring any possible comparison with previous results. It is obviously a scale factor which does not affect the results.

Mode shapes of a continuous beam with a $(n_s - 1)$ intermediate supports will be different from the sinusoidal mode shapes of the simply supported beam. Therefore, for any given number of spans n_s , the normalized abutment reactions will generally be expressed by the general form of Equation (4):

$$\frac{R_{ab,n}}{R_{ab,n}^{SS}} = f_n(\kappa) \frac{M_{eff,n}}{M_{eff,n}^{SS}} \frac{S_a(T_n)}{S_a(T_n^{SS})} = g_n(\kappa) \frac{S_a(T_n)}{S_a(T_n^{SS})} \quad (4)$$

where $f_n(\kappa)$ (or $g_n(\kappa)$) is an unknown function of the normalized support stiffness κ . It is noted that the dependence from n_s has not been formally represented in Equation (4) in order to simplify the notation. While the first two factors in Equation (4) ($f_n(\kappa)$, $M_{eff,n} / M_{eff,n}^{SS}$) depend only on the displacement shape, the latter factor includes the effect of the shape of response spectrum. In the following, for any given number of spans n_s , the three factors $f_n(\kappa)$, $M_{eff,n} / M_{eff,n}^{SS}$ and $S_a(T_n) / S_a(T_n^{SS})$ are plotted first separately and eventually they are combined according to Equation (4). The first two factors have been obtained using numerical models analyzed with OpenSEES (McKenna *et al.* 2004). To generate the normalized spectrum, one of the Italian seismic code spectra is used, corresponding to the site conditions of the sample bridge analysed by means of response history analysis in Della Corte *et al.* (2012). The normalized spectral accelerations are obtained starting with $T_1^{SS} = 1$; further discussion about this aspect is presented later on. In addition, also the normalized periods of vibration, T_n / T_n^{SS} , are plotted in the following in order to generalize and facilitate the comparison of the response spectrum effect. For any given n_s , odd modes till the $(n_s + 1)$ -th are considered in the analysis. This number of modes generally corresponds to a sufficiently large value of the sum of the effective modal mass ratios. Comparisons with the Winkler model are also shown in the following Figures, where dashed lines are used to identify relevant results.

Figure 2 shows the results for the case $n_s = 2$. Figure 2a illustrates the function $f_n(\kappa)$, with $n = 1$ and $n = 3$, i.e. for the first and third vibration modes. From the numerical results shown in Figure 2, it can be argued that the response is characterized by a limit value of κ ($= 200$ based on the results in the Figure), corresponding to a minimum and a maximum of f_n and $M_{eff,n} / M_{eff,n}^{SS}$, respectively. This value

of κ marks the transition from a mode shape exhibiting an appreciable displacement at the intermediate support (small values of κ) to a mode shape with a very small displacement at the intermediate support (large values of κ). Variations of the normalized period of vibration versus the normalized stiffness are shown in Figure 2c, where the Winkler solution is also presented. The Winkler model overestimates the first period of vibration till $\kappa = 300$, while underestimation occurs at larger values of κ . The third period of vibration is always overestimated by the Winkler model in the range of values of κ considered in this study. The normalized spectral accelerations, corresponding to the normalized periods of vibration at any fixed value of κ , are illustrated in Figure 2d. The results are consistent with those of Figure 2c. In fact, first mode spectral accelerations are underestimated for relatively small values of κ , because of the corresponding overestimation of the period of vibration. At relatively large values of κ , though underestimating the first mode period of vibration, there is no overestimation of spectral accelerations because the horizontal plateau of the assumed response spectrum is reached. Third mode spectral accelerations are coincident for the three models for values $\kappa < 200$ because they correspond to the horizontal plateau of the response spectrum. For larger values of κ , there is a reduction of spectral accelerations corresponding to the initial linear branch of the design spectrum, with the lower limit of PGA reached for very small periods of vibration. Differences between the Winkler model and the discrete support system are again explained because of the differences in the periods of vibrations illustrated in Figure 2c.

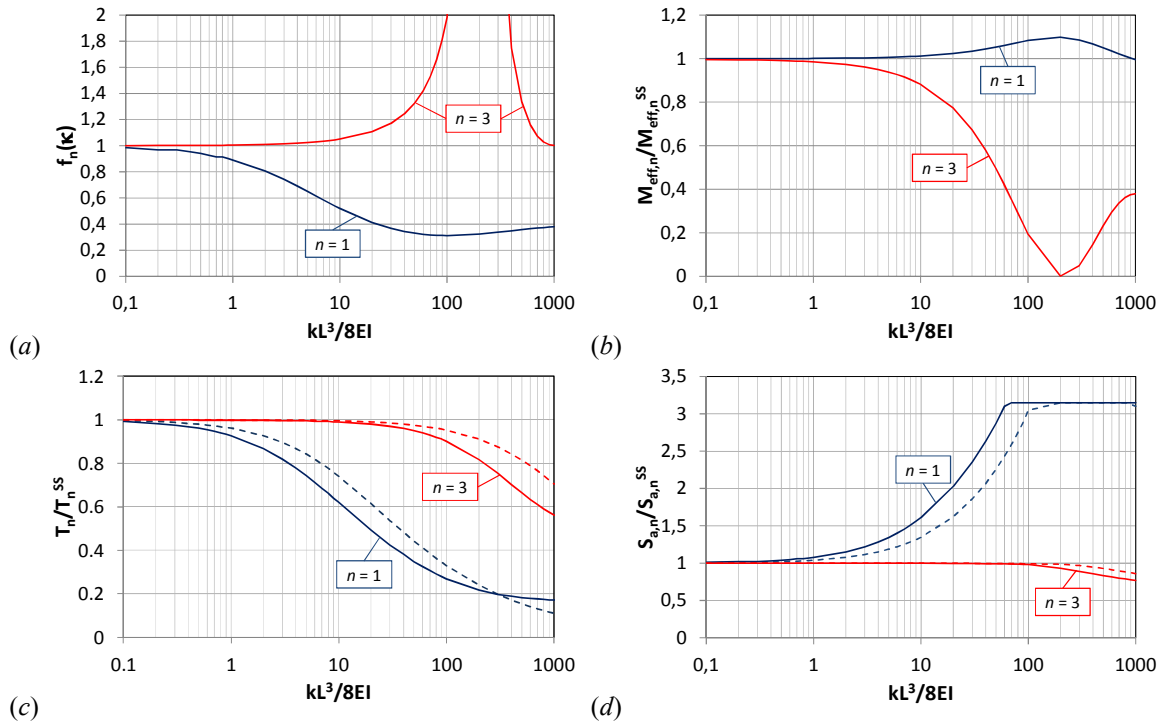


Figure 2. Individual contributions to the normalized abutment reactions; $n_s = 2$: (a) $f_n(\kappa)$; (b) $M_{\text{eff},n}/M_{\text{eff},n}^{\text{SS}}$; (c) T_n/T_n^{SS} ; (d) $S_{a,n}/S_{a,n}^{\text{SS}}$.

Plots similar to those of Figure 2 are reported in Figure 3 for $n_s = 4$. Figures 3a and 3b show that the behaviour exhibited by the third mode in the case $n_s = 2$ is shifted to the fifth mode in the case $n_s = 4$. The limit value of κ is appreciably increased up to values larger than 1000. It is noted also that the first mode exhibit now a shape that is close to the sinusoidal shape over a range of values of κ wider than in the case $n_s = 2$. This can be deduced from the fact that the effective mass of the continuous beam is close to the effective mass of the simply supported beam up to $\kappa = 1000$. The corresponding improvement of the Winkler approximation in predicting periods of vibration and corresponding spectral accelerations is clearly visible in Figures 3c and 3d. However, Figure 3b shows that large differences still persist between effective mass ratios for higher modes of vibration.

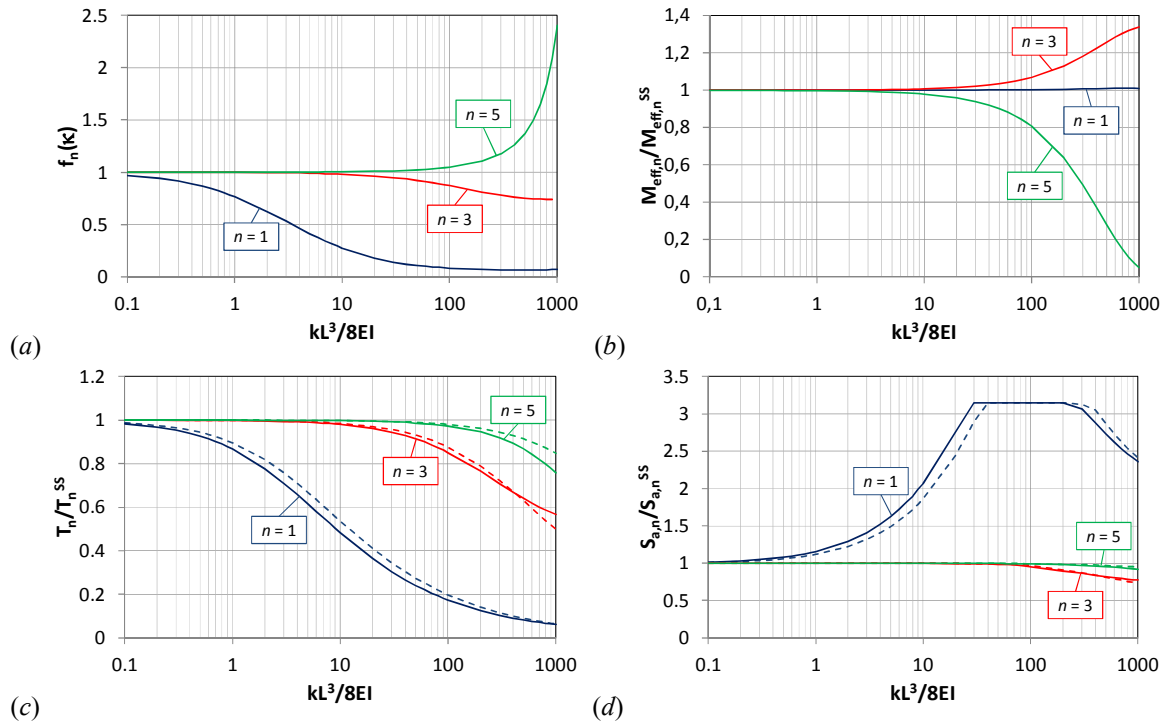


Figure 3. Individual contributions to the normalized abutment reactions; $n_s = 4$: (a) $f_n(\kappa)$; (b) $M_{eff,n}/M_{eff,n}^{SS}$; (c) T_n/T_n^{SS} ; (d) $S_{a,n}/S_{a,n}^{SS}$.

Figure 4 is relevant to the case $n_s = 8$. The comments made with reference to the case $n_s = 4$ can be applied to also the case $n_s = 8$, which confirms the (expected) trend of an improving approximation of the Winkler model when the number of spans is increased. It can be seen from Figure 4c that the effective modal mass ratio is equal to 1 over a wider range of values of κ and a larger number of modes, as respect to the previous cases, what indicates that the displacement shape can be better approximated by a sinusoidal assumption. It is noted that the behaviour exhibited by the third and fifth mode in the cases $n_s = 4$ and $n_s = 8$ is now shifted to the ninth mode.

The product of the function f_n and the effective modal mass ratio, which has been labelled g_n , as well as the product of the three factors highlighted in Equation (4), is shown in Figure 5 for all values of n_s . It is noted that the first factor on the right hand side of Equation (3) is to be directly compared with the more general function g_n , considering that the ratio of the effective masses between the Winkler model and the simply supported beam is equal to unity. Therefore, comparing the numerical solution of the discrete support system with the corresponding Winkler model in terms of the g_n function allows one to capture the effect of the varying shape of the mode of vibration for varying the support stiffness. Such a comparison is presented in the first column of Figure 5, i.e. in Figures 5a, 5c and 5e for $n_s = 2, 4$ and 8 respectively. Large differences can exist between the two models for small values of n_s and/or large values of κ . For sufficiently small values of κ (e.g. smaller than 10), the Winkler model is sufficiently approximate whichever the number of spans is. The differences are also acceptable for $n_s > 8$, whichever is the value of κ but smaller than 100. To establish limit values of κ making acceptable the approximations of the Winkler model requires considering also the errors in the evaluation of periods of vibration, which reflect into different values of spectral accelerations. The effect of the response spectrum can be seen in the second column of Figure 5, i.e. Figures 5b, 5d and 5f for $n_s = 2, 4$ and 8 respectively, where the products of g_n and S_a/S_a^{SS} are plotted. Previous comments are generally confirmed, because the differences exhibited in terms of spectral accelerations can be considered a minor effect as shown by results in Figures 2d, 3d and 4d. The SRSS combination of individual mode contributions shown in Figures 5b, 5d and 5f highlight that the effect of higher modes tend to increase with an increase of the number of spans and the relative support-to-deck stiffness. It has to be noted that the final value of abutment reactions is the product of the ratios shown in Figure 5 and the

corresponding reactions of the simply supported beam. The more flexible is the deck, the larger is the effect of higher modes on abutment reactions of the simply supported beam. Therefore, the effect of higher modes on long continuous beams (i.e. large n_s) is strongly increased because of both the effect on the ratios indicated in Figure 5 and the effect on the reactions of the corresponding simply supported beam.

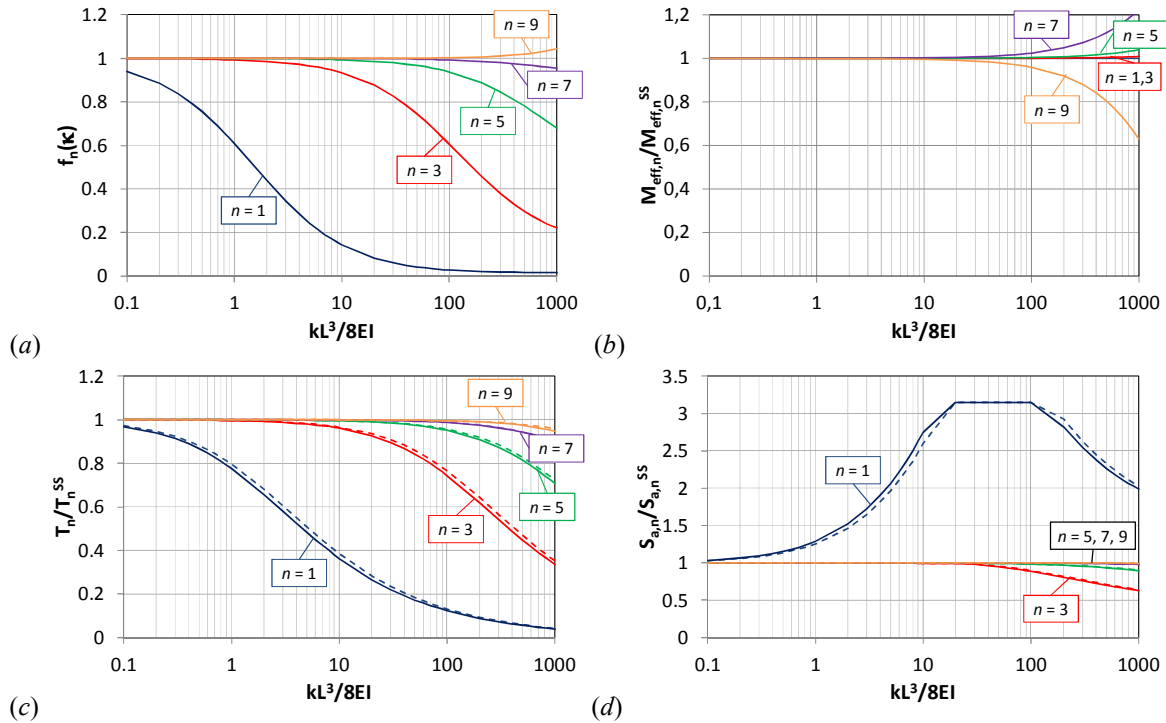


Figure 4. Individual contributions to the normalized abutment reactions; $n_s = 8$: (a) $f_n(\kappa)$; (b) $M_{\text{eff},n}/M_{\text{eff},n}^{\text{SS}}$; (c) T_n/T_n^{SS} ; (d) $S_{a,n}^{\text{SS}}/S_{a,n}$.

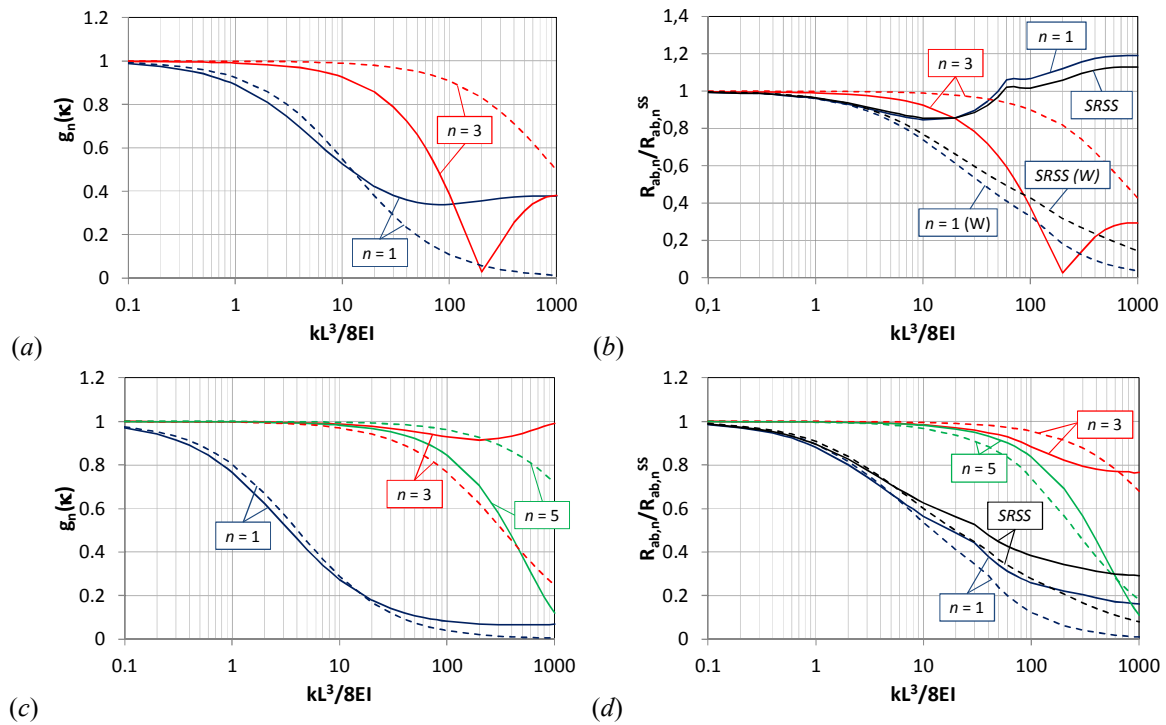


Figure 5. Normalized abutment reactions: $n_s = 2$ (a) and (b); $n_s = 4$ (c) and (d); $n_s = 8$ (e) and (f). (continued)

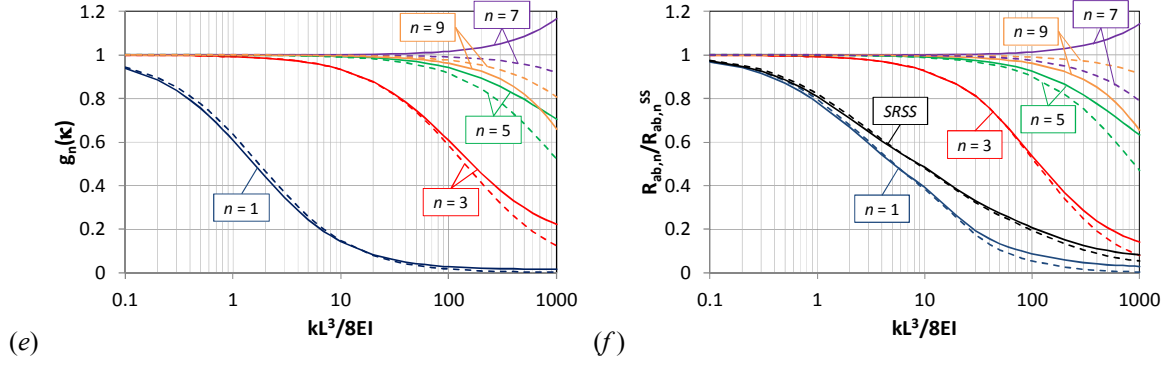


Figure 5. Normalized abutment reactions: $n_s = 2$ (a) and (b); $n_s = 4$ (c) and (d); $n_s = 8$ (e) and (f).

Some of the results shown in Figures 3, 4 and 5 depend on the selected normalized acceleration response spectrum $S_a(T_n)/S_a(T_n^{SS})$. The normalized spectrum was generated assuming $T_1^{SS} = 1$ s and using the corresponding ratios obtained from one selected design spectrum which is currently implemented in the Italian seismic code. Changing this normalized spectrum will obviously change the results that directly depend on it (e.g. the SRSS combination). To generate additional case studies, the first mode period of vibration of the simply supported beam has been subsequently set equal to $T_1^{SS} = 2$ s and $T_1^{SS} = 4$ s. Results similar to the ones already shown for $T_1^{SS} = 1$ s have been obtained.

The effect of the starting value of the first-mode period of vibration of the simply supported beam is illustrated in Figure 6, where a direct comparison between the real beam with discrete support system and the Winkler model is also presented. The horizontal axis of plots in Figure 6 represents values of the parameter $\kappa_s = (n_s - 1)\kappa$, which allows to compare the response of two beams with the same total support stiffness.

Figure 6a illustrates the ratio of first-mode periods of vibration for the two models. Obviously such a ratio does not depend on the assumed T_1^{SS} . Figure 6a clearly highlights that for $n_s = 8$ the Winkler model gives a sufficiently accurate prediction of the first mode of vibration. This is true for also higher modes (not shown in the plots of Figure 6a), as it can be deduced from Figures 2c, 3c and 4c.

The ratio of abutment reactions of the two models is shown in Figure 6b, in terms of SRSS combination of individual modal responses. It can be seen that the abutment reactions changes with the assumed T_1^{SS} when $n_s = 2$ but the response becomes insensitive to T_1^{SS} when $n_s = 8$. Intermediate results are obviously obtained for $n_s = 4$. Such behaviour can be explained with the help of the following Equation (5) and the results discussed previously.

$$\frac{R_{ab,n}}{R_{ab,n}^W} = \frac{f_n(\kappa) M_{eff,n}^{SS} S_a(T_n)}{f_n^W(\kappa) M_{eff,n}^{SS} S_a(T_n^W)} = \frac{g_n(\kappa) S_a(T_n)}{g_n^W(\kappa) S_a(T_n^W)} \quad (5)$$

In Equation (5) $M_{eff,n}^W = M_{eff,n}^{SS}$ and $f_n^W \equiv g_n^W$. The first factor on the right-hand side of Equation (5), i.e. the ratio g_n/g_n^W is only a function of κ , while the second factor, i.e. the ratio $S_a(T_n)/S_a(T_n^W)$, depends also on the assumed T_1^{SS} . In fact, even if the ratio of periods T_n/T_n^W does not depend on T_1^{SS} (Fig. 6a), the ratio of the spectral acceleration depends on it, because the spectrum is generally a nonlinear function of the period of vibration. But, for $n_s = 8$ the approximation $T_n = T_n^W$ holds true (Fig. 6a), thus leading to $S_a \approx S_a^W$ and making the ratio of abutment reactions independent on the selected T_1^{SS} . The ratio of abutment reactions can still be different from unity because of the ratio g_n/g_n^W being different from unity for higher modes of vibration at large values of κ , as shown in Figure 5e. Therefore, though the approximation of the Winkler model improves with increasing the number of spans, underestimation of abutment reactions may still occur for large values of κ .

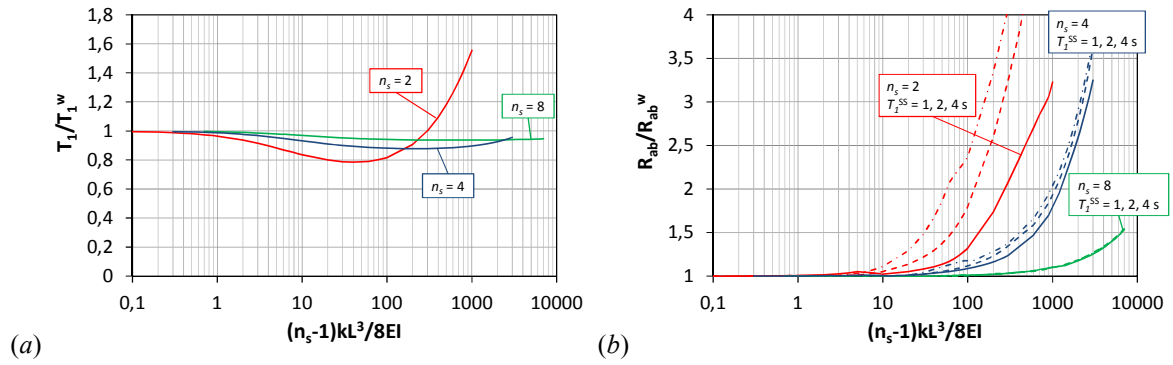


Figure 6. Winkler vs. discrete support system: (a) first period of vibration; (b) abutment reactions.

4. ANALYSIS OF NONLINEAR MODELS

Section 2 has discussed the method to substitute the generally nonlinear structural response with “equivalent” or “effective” linear models. The linear model is “effective” if it allows predicting peak displacement and force demand with sufficient accuracy, at least for design purposes. With reference to the special case of continuous bridges with intermediate supports and abutment restraints, it has been shown that abutment reactions are needed to be evaluated. As a first approximation, the Winkler model was suggested to be used to estimate such reactions. However, Section 3 has shown that in case of linear structural response the Winkler model may underestimate the real abutment reactions. Underestimation can be large for a small number of spans (2 – 4 spans) and/or a large value of the intermediate support stiffness. However, for relatively large values of n_s and/or small values of the normalized stiffness κ the Winkler model may give sufficiently approximate results. Combining the approximations linked to the linearization process and the use of the Winkler model generates a final result that should be assessed by comparing the approximate model results with more rigorous nonlinear finite element model analysis.

Two sample comparisons of this type are presented in Figure 7, with reference to two 13-span bridges with friction pendulum isolation devices on the top of the 12 intermediate piers. The bridge samples are generated from the case study presented in Della Corte *et al.* (2012), by changing the pier stiffness which is assumed equal to either the maximum (Fig. 7a) or the minimum (Fig. 7b) from the initial sample bridge. The two bridges, with large and small values of pier stiffness, were analyzed using a set of 7 ground motions (response history analysis, RHA), by varying the coefficient of friction. The same cases were also analyzed using the simplified procedure outlined at Section 2, using the average spectrum of the 7 records and the CQC modal combination rule (effective response spectrum analysis, ERSA). Peak values of abutment reactions from both RHA (individual points in Figures) and ERSA (continuous lines in Figures) are shown. Figure 7a (large pier stiffness) shows that peak values of abutment reactions from ERSA tend to be smaller than peak values from RHA, if large coefficients of friction are considered. Figure 7b (small pier stiffness) shows instead a good prediction by ERSA for any value of the coefficient of friction. For large values of the coefficient of friction, there is no sliding in the FPS and the bridge behaves as fixed (elastic in the analysis). At such large values of the coefficient of friction, elastic model results similar to those discussed at Section 3 can be used but with reference to the average spectrum of the 7 ground motions and $n_s = 13$. It was found that the Winkler model shall underestimate of about 3% the abutment reactions, at a value of the normalized total pier stiffness of about 2000, which characterizes the bridge with large pier stiffness and large coefficient of friction. From Figure 7a it can be seen that the ERSA method underestimate of about 19% the abutment reactions, which is a significantly larger error. However, it has to be considered that only 7 acceleration records were used for the analysis, whose mean spectrum is characterized by same jagged shape. It is known that using a jagged response spectrum will originate larger errors of the modal combination rules (CQC) as respect to the peaks from RHA results. This is the case of Figure 7a while it is not the case of Figure 7b, because the smaller pier stiffness locates the corresponding bridge into a

region of much more smooth spectral response. Therefore, the 19% underestimation occurring in case of large pier stiffness and large coefficient of friction (Fig. 7a) is attributed to the use of the Winkler model for only 3%, while the remaining 16% of difference is attributed to the use of the statistical combination rule in a case of only 7 ground motions.

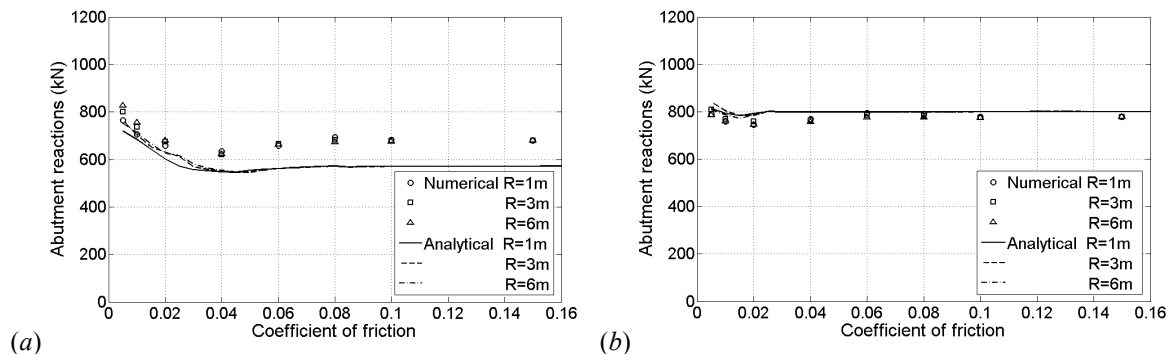


Figure 7. Winkler vs. discrete support system: (a) large pier stiffness; (b) small pier stiffness.

5. CONCLUSIONS

Higher modes of vibration have a significant effect on abutment reactions of continuous bridges. The effect generally increases with increasing number of spans and stiffness of intermediate supports. Using an effective response spectrum analysis (ERSA) method along with an approximate estimate of abutment reactions by means of the Winkler model revealed to work properly in case of bridges with a sufficiently small stiffness of intermediate supports (isolated bridges). However, there will always be an upper bound to the intermediate support stiffness beyond which the error linked to the Winkler model will start to increase significantly and to become unacceptably large.

REFERENCES

- AASHTO (2010). *Guide specifications for seismic isolation design*. American Association of State Highway and Transportation Officials, Third Edition, July 2010.
- CEN (2005). *Eurocode 8. Design of structures for earthquake resistance – Part 2: Bridges*. (EN 1998-2 2005). European Committee for Standardization, Brussels.
- Chopra, A.K., Goel, R.K. (2002). A modal pushover analysis procedure for estimating seismic demands for buildings. *Earthquake Engineering and Structural Dynamics*, **31**, 561-582.
- Della Corte, G., De Risi, R., Di Sarno, L. (2012). Transverse seismic response of partially-isolated continuous bridges with friction-pendulum devices. *5th European Conference on Structural Control*, 18-20 June, Genoa, Italy.
- Dwairi, H.M., Kowalsky, M.J. (2004). Investigation of the Jacobsen's equivalent viscous damping approach as applied to displacement-based seismic design. *Proceedings of the 13th World Conference on Earthquake Engineering*, Vancouver, B.C. Canada, Paper No. 228, CD-ROM.
- Makris, N., Kampas, G., Angelopoulou D. (2010). The eigenvalues of isolated bridges with transverse restraints at the end abutments. *Earthquake Engineering and Structural Dynamics*, **39**, 869-886.
- McKenna, F., Mazzoni, S., Scott, M.H., Fenves, G.L. (2004). *Open System for Earthquake Engineering Simulation (OpenSEES) (version 1.7.4)*. Pacific Earthquake Engineering Research Center, University of California at Berkeley, <http://opensees.berkeley.edu>.
- Paraskeva, T.S., Kappos, A.J. (2010). Further development of a multimodal pushover analysis procedure for seismic assessment of bridges. *Earthquake Engineering and Structural Dynamics*, **39**, 211-222.
- Priestley, M.J.N., Calvi, G.M., Kowalsky, M.J. (2007). *Displacement based seismic design of structures*. IUSS Press, Pavia.
- Tsai M.-H. (2008). Transverse earthquake response analysis of a seismically isolated regular bridge with partial restraint. *Engineering Structures*, **30**, 393-403.
- Tubaldi, E., Dall'Asta, A. (2011). A design method for seismically isolated bridges with abutment restraint. *Engineering Structures*, **33:3**, 786-795.